Enhancing the Magnetoviscosity of Ferrofluids by the Addition of Biological Nanotubes

Zhenyu Wu,[†,⊥] Anna Mueller,[‡,⊥] Sven Degenhard,[‡] S. Emil Ruff,[‡] Fania Geiger,[‡] Alexander M. Bittner,[§] Christina Wege,[‡,*] and Carl E. Krill III[†,*]

[†]Institute of Micro and Nanomaterials, Ulm University, Albert-Einstein-Allee 47, 89081 Ulm, Germany, [‡]Department of Molecular Biology and Virology of Plants, Institute of Biology, Universität Stuttgart, Pfaffenwaldring 57, 70569 Stuttgart, Germany, and [§]CIC nanoGUNE Consolider, Tolosa Hiribidea 76, 20018 Donostia—San Sebastian, and IKERBASQUE, Basque Foundation for Science, 48011 Bilbao, Spain. [⊥]These authors have contributed equally to this work.

ABSTRACT Applying a magnetic field to many ferrofluids leads to a significant increase in viscosity, but the phenomenon has yet to find technological exploitation because of the thinning caused by even weak shear flows. We have discovered that the addition of plant-virus-derived nanotubes to a commercial ferrofluid can give rise to a dramatic enhancement in magnetoviscosity and a suppression of shear thinning. The dependence of this effect on nanotube aspect ratio and surface charge, both of which were varied biotechnologically, is consistent with a "scaffolding" of magnetic particles into quasi-linear arrays. Direct support for this explanation is derived from transmission electron micrographs, which reveal a marked tendency for the magnetic nanoparticles to decorate the outside surface of the virus nanotubes.

KEYWORDS: ferrofluid · TMV-like particles · bioengineering · magnetoviscosity · nanocomposite · biotemplate

Initially prepared in the 1960s, ferrofluids represent perhaps the first commercially viable example of a nanocomposite material, combining the magnetic properties of ferrimagnetic (or ferromagnetic) nanoparticles with the fluid properties of the carrier liquid in which the particles are suspended.[1] Owing to the high magnetic susceptibility of such suspensions, they can be held in place and manipulated by externally applied magnetic fields. This unique feature has led to a variety of novel applications, such as using ferrofluids to create low-friction, vacuum-tight seals around rotating shafts (in hard disk drives, for example) or to transfer heat from the voice coils of high-power loudspeakers. In recent years, ferrofluids have received increasing attention for their potential use in biomedical applications, such as cell labeling, site-specific drug delivery, magnetic hyperthermia, or the magnetic filtration of pathogens from liquid suspensions.[2−4]

Ultimately, the technological potential of ferrofluids relies on the nature of the coupling between the suspended magnetic nanoparticles and the hydrodynamics of the surrounding liquid. This coupling can be so strong that even modest externally applied magnetic fields suffice to increase the viscosity of the ferrofluid by orders of magnitude.[5,6] This so-called *magnetoviscous effect* is generally attributed to the magnetic-field-induced formation of chain-like agglomerates of nanoparticles, which align themselves with the applied field and hinder the flow of carrier fluid in the transverse direction.[7−12] Indeed, in *magnetorheological (MR) fluids*—liquid suspensions of magnetic particles 2−3 orders of magnitude larger than those of ferrofluids—the formation of such chains has been demonstrated experimentally.[13] The magnetoviscosity of MR fluids is so strong that it has found commercial use in electromagnetically switchable shock absorbers in automobiles, vibration dampers for suspension bridges, and (potentially) aircraft landing gear.[14−16] However, owing to the micrometer size of the suspended magnetic particles, MR fluids are prone to sedimentation, which must be counteracted by actively pumping the fluid. In contrast, Brownian motion alone suffices to keep the much-smaller particles of a ferrofluid suspended indefinitely, thus obviating the need to maintain steady flow. For the same reason, ferrofluids are less susceptible to agglomeration than are MR fluids, suggesting that the magnetoviscosity of a ferrofluid has the potential for much better long-term stability.

Despite these apparent advantages, there has been virtually no commercial exploitation of ferrofluid magnetoviscosity to date. This fact can be attributed to the substantial decrease in magnetoviscosity that ferrofluids suffer when subjected to shear

*Address correspondence to carl.krill@uni-ulm.de, christina.wege@bio.uni-stuttgart.de.

Received for review March 30, 2010 and accepted July 12, 2010.

Published online July 22, 2010. 10.1021/nn100645e

forces, as the latter are able to overcome the weak interactions holding the chain-like nanoparticle clusters together, thus breaking them apart and thwarting the mechanism for viscosity enhancement. This explanation for *shear thinning* is consistent with the predictions of computer simulations,[8−10] and it has gained experimental support from recent small-angle neutron scattering investigations as well.[11,12]

Birringer *et al.*[17] proposed a novel strategy for overcoming this problem: if the loosely bound nanoparticle chains of a conventional ferrofluid were replaced with stiff magnetic nanorods or nanotubes, then the resulting ferrofluid ought to retain its field-induced viscosity enhancement even at high shear rates. Not only would aspherical magnetic nanoparticles be expected to impart a higher viscosity when held in place by an applied magnetic field,[18] but they would also not lose their shape anisotropy in the event of shearing forces,[17] as is the case with fragile agglomerates. A further practical advantage of permanent shape anisotropy might be its contribution to overcoming the superparamagnetic limit of individual nanoparticles,[19] which holds the promise of imparting a stronger magnetic field response (but also may exacerbate the challenge of stabilizing the suspended particles against agglomeration).

Here, we report our first efforts to implement the strategy proposed in ref 17, albeit in an approximate—yet surprisingly effective—manner. Since $10^{15}-10^{17}$ nanoparticles are typically suspended in a milliliter of a conventional ferrofluid, in order to prepare a "nanorod ferrofluid" one must employ a fabrication route with the potential for large-scale production of aspherical nanomagnets. Candidate techniques include aerosol condensation,[17,20] liquid-phase chemical reaction,[21,22] deposition in nanoporous templates,[23,24] and the hybridization of spherical nanoparticles with aspherical objects, such as carbon nanotubes (CNTs).[25] The latter method is particularly promising as a relatively low-cost approach; however, before magnetic particles can be attached to the surface of a CNT, the hydrophobic nature of the CNT and its chemical inertness must be overcome by careful functionalization. A simpler alternative might be offered by mechanically stiff nanotubes having exposed functional chemical groups on their outer surfaces. This is the approach adopted in this article, in which we report the first use of an intrinsically functionalized, tube-shaped nanoparticle—the *Tobacco mosaic virus* (TMV)—and of TMV-derived biotechnologically tailored nanotubes of altered length and modified surface charge as additives for enhancing the rheological properties of a conventional ferrofluid.

Tobacco mosaic virus (TMV) is a biomolecule complex that forms naturally in the shape of a 300 nm-long nanotube with outer and inner diameters of 18 and 4 nm, respectively. The virus is widespread in different plant species (and in most types of cigarettes), accumulates to high amounts and does not infect animals. Each TMV particle consists of 2130 identical coat protein (CP) subunits that self-assemble around a strand of RNA either during plant cell infection or *in vitro* under chemically controlled conditions.[26,27] The structure of TMV and its physicochemical properties are well understood.[28,29] By modifying the length of the encapsidated RNA strand, one can tailor the aspect ratio of the resulting artificial noninfectious TMV-like particles to values larger or smaller than that of natural TMV;[30] likewise, genetic engineering techniques make it possible to modify the CP subunits themselves, enabling TMV variants to be prepared with altered surface chemistries.[31−33] For a biological specimen, the virus is unusually stable, withstanding temperatures up to 80 °C and pH values from below 3 to 9.[34−36] Owing to these properties, TMV has become a popular subject of nanotechnological experimentation, serving as a template for the directed deposition of metals,[34,37−40] as a vessel for controlled chemical reactions,[41] and as a building block for the assembly of three-dimensional nanoarrays.[32,42,43] In one study,[44] TMV particles were even deliberately introduced into a ferrofluid in a similar manner as reported below, but not with the aim of enhancing any properties of the ferrofluid; rather, the authors required a parallel alignment of a large number of TMV particles—a goal that they achieved by applying a magnetic field to the TMV/ferrofluid sample.

RESULTS AND DISCUSSION

Small concentrations of aspherical TMV—or TMV-derived—particles were synthesized in three different size classes (lengths of approximately 90, 170, and 300 nm) and systematically analyzed for their capacity to modify the rheological properties of a ferrofluid. To obtain a deeper understanding of the observed effects, the protein surface of the bioadditive nanotubes was modified by genetic engineering into two further variants, TMV_{Cys} and TMV_{Lys}. All TMV samples were mixed into a commercially available ferrofluid, LCE-25 (*SusTech* GmbH, Germany), which consists of cobalt ferrite ($CoFe_2O_4$) nanospheres (ϕ 10−18 nm) suspended in a solution of diethylene glycol and DI water. The magnetoviscosity of the resulting TMV/ferrofluid mixtures was measured as a function of additive concentration and vibrational frequency.

Figures 1−3 illustrate the effect of TMV-based additives on the rheological properties of LCE-25 ferrofluid. In Figure 1a,b, the imaginary part G'' of the complex modulus G^* and the real part η' of the complex viscosity η^* of LCE-25/TMV ferrofluids are plotted against vibrational frequency—both with and without an applied magnetic field—and compared to the viscosity of pure LCE-25. At zero applied field, the addition of TMV had no effect on G'', which is a measure for the dissipation of energy in the fluid, or on the viscosity η'. But at 110 mT, G'' increased by an order of magnitude in the

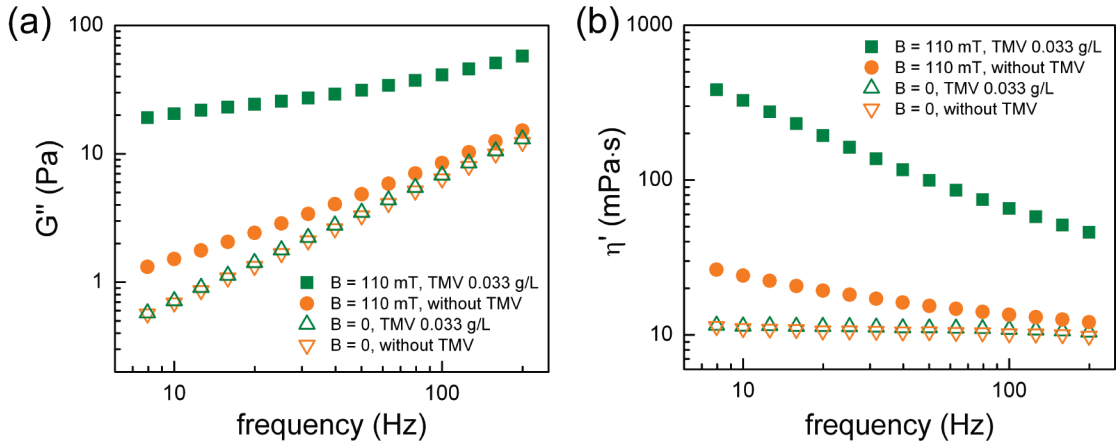

Figure 1. (a) The modulus G'' and (b) the viscosity η' plotted as a function of vibrational frequency for diluted LCE-25 ferrofluids with and without TMV additive (0.033 μg TMV/μL ferrofluid). Open symbols denote zero applied magnetic field, and closed symbols correspond to $B = 110$ mT.

sample containing virus particles, and, consequently, the fluid was about 10 times more viscous than the pure ferrofluid. This enhancement persisted over the entire frequency range, which is indicative of an improved stability even at high shear rates (see Supporting Information). The change in viscosity was fully reversible upon switching the magnetic field on and off many times (see Supporting Information), and the effect was stable upon storing the sample under ambient conditions for months.

Varying the concentration of TMV in the ferrofluid had no discernible effect on the viscosity at zero applied magnetic fields, but both η' and the imaginary part of the complex viscosity, η'' increased strongly with TMV concentration as the magnetic field strength was raised (Figure 2).

To test whether the magnetoviscosity depends on the aspect ratio of the TMV additive, ferrofluids containing virus-like particles ~170 or ~90 nm in length were prepared and tested. Transmission electron microscopy (TEM) was used to establish that the length distribution of the additive particles was narrow.[30] The strength of the magnetoviscous effect at a given magnetic field B can be expressed by the ratio

$$\frac{\Delta\eta'}{\eta'_0} = \frac{\eta'(B) - \eta'(B=0)}{\eta'(B=0)} \quad (1)$$

in which η'_0 denotes the real part of the complex zero-field viscosity. When we measured this ratio as a function of B (Figure 3), we discovered that, although LCE-25 ferrofluid by itself manifested only a small viscosity increase with applied magnetic field (filled diamonds), the addition of virus particles always led to significant viscosity enhancement. Furthermore, the relative viscosity scaled roughly linearly with magnetic field strength for all virus lengths, and, at a given magnetic field, the magnetoviscosity grew with TMV length, reaching 2800% at $B = 110$ mT and $f = 10$ Hz for the sample containing 300 nm-long virus particles.

Direct imaging of dried LCE-25/TMV mixtures was carried out by TEM. The images shown in Figure 4 provide graphic evidence for an attractive interaction between LCE-25 nanoparticles and plant viral tubes.

How is it possible for small concentrations of a nonmagnetic bioadditive to have such a strong impact on a ferrofluid property like magnetoviscosity, which seems like it should depend almost entirely on the size and concentration of the suspended magnetic particles? Figure 4c offers a tantalizing explanation: Here, the TMV particles appear to be acting as the "scaffolds" of a roughly linear arrangement of magnetic particles over the length of the virus, thereby generating rodlike magnetic structures that might be expected to induce significant viscosity enhancement. Such linear aggregation of magnetic nanoparticles is completely absent in TEM images recorded from samples without TMV (*e.g.*, Figure 4a). The most likely explanation for this finding is the existence of an attractive interaction between magnetic nanoparticles and TMV, perhaps having its origin in an electrostatic attraction between the negatively charged ferrofluid constituents[45] and the exterior sur-

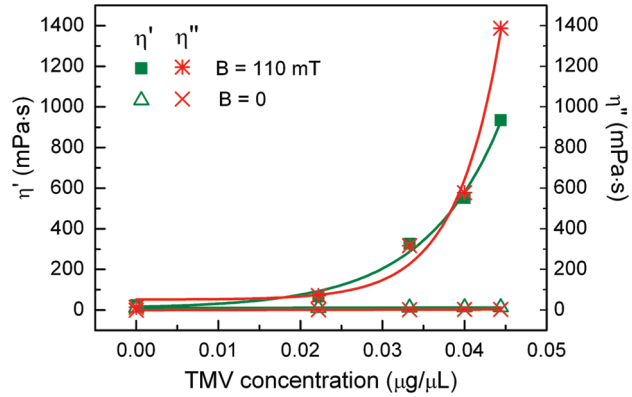

Figure 2. The viscosities η' and η'' of LCE-25/TMV mixtures plotted against TMV concentration for zero magnetic field and $B = 110$ mT. All measurements were carried out at a vibrational frequency of 10 Hz. The smooth curves drawn through the data points are guides to the eye.

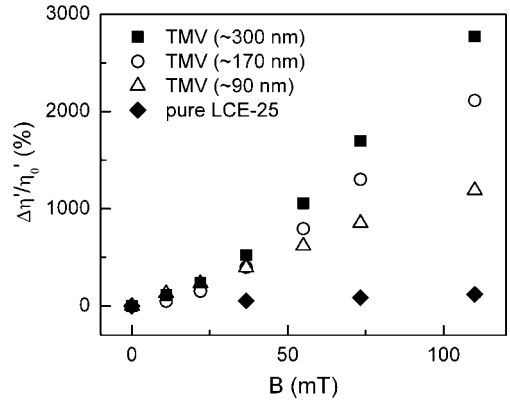

Figure 3. Relative viscosity (referenced to the value at $B = 0$) plotted against applied magnetic field for LCE-25/TMV ferrofluids containing TMV particles of various lengths (virus particle concentration, 0.033 μg/μL). All measurements were carried out at a vibrational frequency of 10 Hz.

face of the virus, which contains positively charged patches. As a nucleoprotein complex, TMV is composed of amino acids arranged in such a manner that the outer surface exposes side chains including polar groups of various charges, which depend to a certain extent on the pH of the surrounding solution.[28] At the pH employed in our experiments (about 5), there is evidence that the net charge of the outer accessible TMV surface is positive,[38,39] despite the presence of interspersed—but less-exposed—negative patches. In previous investigations of the electroless deposition of metals like Co, Ni, Ag, or Au on TMV, the electrostatic interaction between negatively charged ions and the positively charged TMV surface was exploited in order to initiate metal deposition.[34,38] In our case, the magnetic particles of the conventional ferrofluid may attach to TMV for a similar reason, with hydrogen bridging making an additional contribution to the stability of the TMV/nanoparticle complex.

Support for this hypothesis comes from a set of measurements in which we compared the influence on magnetoviscosity of TMV variants having altered amino acid compositions. The surface of TMV_{Lys} is significantly more positively charged than that of TMV_{Cys} and natural TMV (Figure 5), implying that TMV_{Lys} would interact more strongly with negatively charged $CoFe_2O_4$ nanoparticles. The magnetoviscous effect induced by TMV_{Lys} was indeed found to exceed that of TMV_{Cys} and natural TMV at the same TMV concentration level. Addition of TMV_{Cys} to the LCE-25 ferrofluid had a comparable effect on the magnetoviscosity as natural TMV, which again is consistent with the supposition that electrostatic interactions are primarily responsible for TMV/nanoparticle complex formation.

Additional support for the scaffolding model comes not only from the length dependence evident in Figure 3—longer virus particles impart a greater viscosity enhancement, as expected theoretically[46]—but also from measurements of the viscosity of LCE-25/TMV ferrofluids in which the TMV concentration was held constant at 0.033 μg/μL while the concentration of $CoFe_2O_4$ particles was varied from zero to 0.7 vol %. A plot of magnetoviscosity as a function of the volume fraction of magnetic particles (Figure 6) manifests two distinct regions: at low volume fractions the magnetoviscosity increases much faster with the number of $CoFe_2O_4$ particles per unit volume than in control samples containing no TMV; however, beyond a critical magnetic concentration of about $c_c = 0.063$ vol %, the slope of the magnetoviscosity *versus* concentration curve is unaffected by the presence of TMV. Evidently, above c_c each "excess" magnetic particle makes the same contribution to the overall magnetoviscosity as in pure LCE-25 ferrofluid, whereas the viscosity enhancement per magnetic particle is many times larger at concentrations below c_c.

We attribute this observation to the scaffolding of up to 0.063 vol % magnetic particles into quasi-linear aggregates by TMV, an effect that must saturate once the virus' capacity for taking on additional magnetic particles has been exhausted. At c_c, there are about 720 $CoFe_2O_4$ nanoparticles present in the sample for each TMV, but geometrical considerations indicate that single monolayer coverage would correspond to the attachment of only ~140 magnetic particles. Hence, our interpretation of Figure 6 requires an effective attraction of roughly five monolayers of magnetic particles to each TMV nanotube, which seems plausible in light of the multilayered aggregation evident at the viral surfaces shown in Figure 4. Below saturation, the growth in size and number of TMV/nanoparticle complexes

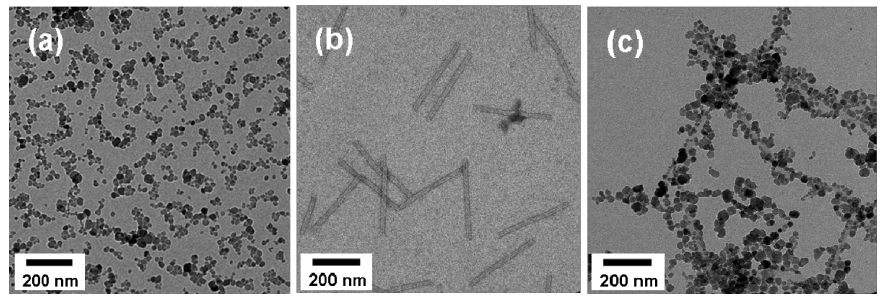

Figure 4. Bright-field TEM micrographs of (a) pure LCE-25 ferrofluid, showing the $CoFe_2O_4$ nanoparticles that remain after drying the carrier fluid; (b) TMV particles prior to suspension in the ferrofluid; and (c) the LCE-25/TMV mixture. In image c, the magnetic nanoparticles are seen to have clustered preferentially on the surface of the virus particles.

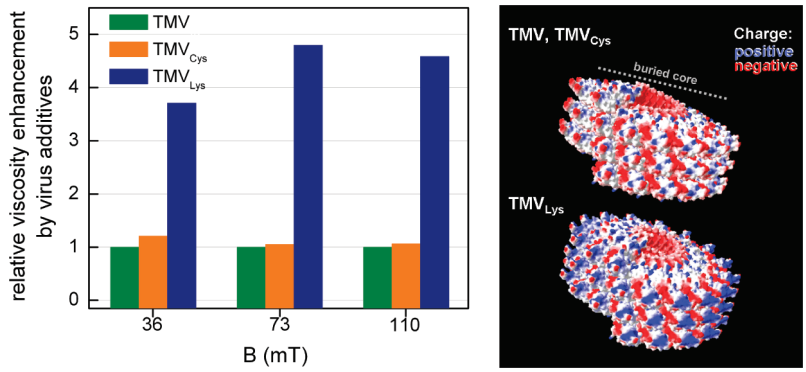

Figure 5. (Left) Relative viscosity enhancement (referenced to samples with natural TMV additive) plotted as a function of the applied magnetic field for ferrofluids containing identical concentrations of TMV, TMV$_{Cys}$, and TMV$_{Lys}$. All TMV variants were ~300 nm in length, and all viscosity measurements were carried out at 10 Hz. (Right) Atomic models indicating the electrostatic potential calculated for the distinct TMV variants of this study. Positive charge is shown in blue and negative charge in red. For natural TMV, despite the presence of interdispersed negative patches, a positive net charge of the accessible, protruding surface domains is expected in the pH range employed in the experiments. In TMV$_{Lys}$, lysine residues were introduced at the C-terminus of the coat protein, resulting in additional positively charged amino groups on the outer protein shell. In contrast, replacement of a serine at the surface of the coat protein by a thiol group-containing cysteine (mutant TMV$_{Cys}$) does not alter the charge to a significant extent.

with increasing magnetic volume fraction offers a ready explanation for the steep slope of the magnetoviscosity curve of Figure 6, as previous studies of ferrofluids containing a broad distribution of magnetic particle sizes have found that magnetoviscosity is determined primarily by the larger particles in the sample—even when smaller particles are present in far greater number.[47,48]

If the magnetoviscosity scaled simply with the number of (saturated) TMV/nanoparticle complexes per unit volume, however, then we would expect a strictly linear dependence of viscosity on TMV concentration. Figure 2 indicates that linear extrapolation of low-virus-concentration magnetoviscosity levels strongly underestimates the viscosity at higher TMV concentrations. If this measurement had been performed on a conventional ferrofluid, then the upward curvature of an η' *versus* concentration plot would most likely be attributed to interactions between magnetic particles, which become more probable as the average particle spacing decreases. Analogous argumentation applied to LCE-25/TMV ferrofluids would entail that the upward curvature in η' results from interactions among TMV/nanoparticle complexes, the likelihood of which increases as the volume fraction of TMV is raised. Extensive interaction among complexes may be viewed as an example of "network formation," which typically manifests itself during a viscosity measurement through a significant increase in the magnitude of the imaginary part of the complex viscosity, η''.[18] For the sample of Figure 2, η'' is seen to grow rapidly with TMV concentration, implying that the development of an internal microstructure in the LCE-25/TMV suspension is responsible for virus-induced viscosity enhancement.

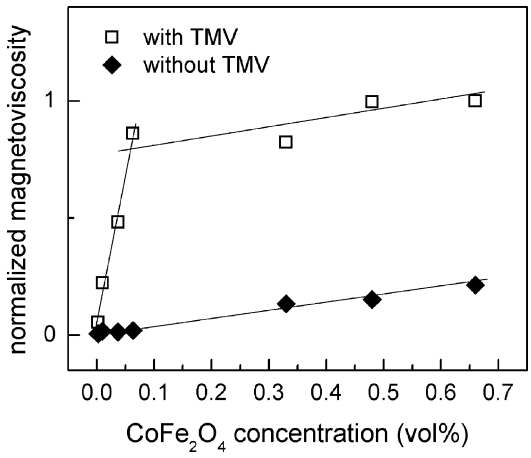

Figure 6. Normalized magnetoviscosity of ferrofluids with and without TMV plotted against $CoFe_2O_4$ particle concentration. The TMV concentration was 0.033 μg/μL for all samples containing virus nanotubes. All measurements were carried out at a vibrational frequency of 10 Hz and an applied magnetic field of 110 mT.

This has important consequences for the proper interpretation of the length dependence seen in Figure 3: on the one hand, the observed increase in magnetoviscosity with TMV length could arise from longer quasi-one-dimensional magnets being held more securely in orientation by the applied magnetic field; on the other hand, longer TMV/nanoparticle complexes might find it easier to form networks, particularly if the stability of the latter is promoted by entanglement of the rodlike structures. (Note that the samples in Figure 3 each have the same TMV mass concentration, meaning that about three times as many ~90 nm TMV particles were present per unit volume as ~300 nm TMV. If comparison is made between specimens of equal TMV particle number concentrations, then the differences in magnetoviscosity are even greater than those evident in the figure.) However, it is clear from the reversibility of the measured magnetoviscosity (see Supporting Information) that the network is stable only in the presence of an applied magnetic field, which rules out the irreversible formation of a gel-like microstructure.

In conclusion, through the addition of small amounts of *Tobacco mosaic virus* (TMV), the magnetoviscous effect of a conventional cobalt ferrite-based ferrofluid was enhanced by more than one order of magnitude. The TMV-induced viscosity enhancement scales roughly linearly with the applied magnetic field, but nonlinearly with virus concentration. A consistent correlation between the length of the nanotubes comprising the virus-derived additive and the magnitude of the resulting magnetoviscosity was also observed. The surface functional groups of TMV appear to be responsible for an electrostatic interaction with the $CoFe_2O_4$ particles, leading to the formation of quasi-linear aggregates of magnetic nanoparticles attached to the tube-shaped virions. We postulate that alignment of these rodlike magnetic structures in an applied magnetic field leads to viscosity enhancement in much the same way that dynamically formed chains of nanoparticles are thought to account for the magnetoviscosity of conventional ferrofluids. Since the TMV-based structures are much longer in length and mechanically far more stable, however, the resulting viscosity enhancement is correspondingly greater and is less susceptible to shear thinning.

With this new class of ferrofluids it may now be possible to impart precisely controlled, rapidly switchable damping forces to moving parts, particularly in micromechanical devices. Moreover, the nonlinear increase of viscosity with TMV concentration could be exploited, for instance, by using magnetic fields to induce enrichment of the TMV/nanoparticle complex concentration, thus localizing the viscosity increase within a given region, perhaps down to micrometer dimensions. The consistent effects obtained from virus-like particles that were engineered to change the aspect ratio or the surface charge demonstrates the immense tailoring potential of biotechnology for technological applications. One such approach that may be of direct benefit to magnetic fluids would be the development and production of biobased additive powders, which could be used to regulate and improve fluid properties on a larger scale.

EXPERIMENTAL METHODS

Ferrofluid. A commercially available ferrofluid LCE-25 (*SusTech* GmbH, Germany) was adopted. LCE-25 consists of cobalt ferrite ($CoFe_2O_4$) nanospheres (ϕ 10−18 nm) suspended in diethylene glycol. The surfaces of the nanoparticles are negatively charged;[45] consequently, agglomeration of nanoparticles is prevented electrostatically without recourse to surfactant molecules. Commercial samples can be diluted by the addition of diethylene glycol and deionized water (DI water) without disturbing the colloidal stability. In our experiments, we diluted LCE-25 to 10 times the original volume, obtaining a ferrofluid with a solid volume fraction of 0.66%, corresponding to a weight fraction of 3.1% of the magnetic phase. Even at such a low concentration, a considerable degree of particle−particle interaction can be expected, which may promote the formation of microstructural features like particle chains in the presence of a magnetic field. To maintain the colloidal stability of the ferrofluid, the pH value of the samples was kept at about 5 in all experiments.

TMV Preparation. TMV particles were purified from systemically infected tobacco plants (*Nicotiana tabacum* cv Samsun nn) as described in ref 49. The virion concentration was determined by UV spectrophotometry[50] and by SDS-polyacrylamide gel electrophoresis, according to standard procedures.[51] Aliquots containing 10, 20, 30, 45, or 90 μg TMV in sodium potassium phosphate buffer (10 mM, pH 7.2) were dialyzed against H_2O using Slide-a-Lyzer MINI dialysis units (Pierce) for 2 h at room temperature. Subsequently, the solutions were frozen in liquid nitrogen and freeze-dried for 4 days. The appropriate amount of diluted LCE-25 ferrofluid was added to a vial containing TMV powder to obtain the desired final TMV concentration. The resulting LCE-25/TMV mixture was subjected to an ultrasonic bath for 5 min to ensure a homogeneous dispersion of TMV particles in the carrier fluid. TMV-like tubes with different aspect ratios were synthesized *in vitro*, using three different types of RNA governing the length of the products obtained *via* self-assembly reactions. Applying a procedure described in detail elsewhere,[30] TMV-like nanotubes were generated in distinct size ranges, with predominant lengths of about 300 nm (with RNA of 6395 nucleotides [nt]), 170 nm (with RNA of 3651 nt) and 90 nm (with RNA of 1860 nt), respectively. Additionally, ferrofluids containing two kinds of genetically engineered TMV variants of altered protein shells—LCE-25/TMV_{Lys} and LCE-25/TMV_{Cys} (unpublished data, to be described elsewhere), both about 300 nm in length—were prepared using RNA of 6395 nt. The particles of TMV variant TMV_{Lys} expose one additional lysine residue on the outer surface of each CP subunit (*i.e.*, ∼2300 lysine residues per particle). Lysine harbors a protonated amino function under the conditions employed in this study; consequently, this TMV variant carries a more positive surface charge than natural TMV. In contrast, TMV_{Cys} exposes one cysteine residue per CP subunit, the thiol function of which is not expected to modify the surface charge in LCE-25 ferrofluid to a major extent.

Magnetoviscosity Measurements. The dynamic viscosity of the LCE-25/TMV composites was measured in compression using a piezo-membrane axial vibrator (PMAV, IdM Ulm, Germany), which is designed for the characterization of sample volumes as small as 50 μL.[52,53] In this apparatus, the sample is confined between two horizontal plates (ϕ 20 mm), the lower of which is forced to vibrate (amplitude <5 nm) by a piezoelectric actuator at driving frequencies between 8 and 200 Hz. The response of the overall system (sample + plates) is detected by a piezoelectric sensor and converted into the complex modulus G^*, from which the complex viscosity of the sample η^* is calculated (see Supporting Information for details), after excluding the contribution of the plates by an empty measurement. By means of an electromagnetic coil, the sample can be subjected to axial magnetic fields as strong as 110 mT. Despite the inhomogeneous shearing inherent to the "squeeze-flow" geometry of this instrument, the technique provides quantitatively reliable data for polymer solutions and colloidal suspensions.[53] The reproducibility of viscosity measurements was better than 0.3 mPa · s.

TEM Characterization. Samples were placed on Formvar-carbon-coated copper grids (300 mesh), washed with DI water, and negatively stained with uranyl acetate (2%) in order to improve the contrast of the TMV particles. Images were recorded with a FEI TECNAI G20 transmission electron microscope operated at 120 kV.

TMV Atomic Models. The structure of the TMV coat protein helix was taken from the Protein Data Bank at Brookhaven (PDB entry code 2OM3 resolution, 4.4 Å as obtained by high-resolution cryo-EM), and extended to the C-terminus of the TMV constructs used. The protein structure was visualized using Swiss-PdbViewer 4.0.1; energy minimization was performed with the GROMOS96 implementation of PdbViewer.

Acknowledgment. We are indebted to P. Martinoty (U. Strasbourg), H. Jeske (U. Stuttgart), and M. Knez (MPI Halle) for help-

ful and supportive discussions. We also thank S. Nussberger, M. Schweikert, and A. G. Heyer for providing access to the TEM and lyophilization facilities in Stuttgart; L. Bogani for facilitating microscopy experiments and helpful advice; F. Eber for sample preparation support; S. Kober for virus isolation; S. Eiben for help with the adaptation and visualization of atomic models; and H.-M. Sauer (SusTech GmbH) for kindly providing the samples of LCE-25 ferrofluid and technical information. Finally, we gratefully acknowledge financial support for this project from the Deutsche Forschungsgemeinschaft (DFG) through Research Priority Program 1165 and subsidiary support from the Baden-Württemberg-Stiftung.

Supporting Information Available: Notes on the real and imaginary parts of the complex viscosity, frequency dependence of the magnetoviscous effect, reversibility of the measured magnetoviscosity, genetically engineered TMV variants with altered surfaces, and visualization of TMV/ferrofluid microstructures using optical microscopy. This material is available free of charge *via* the Internet at http://pubs.acs.org.

REFERENCES AND NOTES

1. Papell, S. S. Low Viscosity Magnetic Fluid Obtained by the Colloidal Suspension of Magnetic Particles. U.S. Patent 3 215 572 1964.
2. Jeong, U.; Teng, X.; Wang, Y.; Yang, H.; Xia, Y. Superparamagnetic Colloids: Controlled Synthesis and Niche Applications. *Adv. Mater.* **2007**, *19*, 33–60.
3. Son, S. J.; Bai, X.; Lee, S. B. Inorganic Hollow Nanoparticles and Nanotubes in Nanomedicine: Part 1. Drug/Gene Delivery Applications. *Drug Discovery Today* **2007**, *12*, 650–656.
4. Xu, C.; Sun, S. Monodisperse Magnetic Nanoparticles for Biomedical Applications. *Polym. Int.* **2007**, *56*, 821–826.
5. Rosensweig, R. E.; Kaiser, R.; Miskolczy, G. Viscosity of Magnetic Fluid in a Magnetic Field. *J. Colloid Interface Sci.* **1969**, *29*, 680–686.
6. McTague, J. P. Magnetoviscosity of Magnetic Colloids. *J. Chem. Phys.* **1969**, *51*, 133–136.
7. Butter, K.; Bomans, P. H. H.; Frederik, P. M.; Vroege, G. J.; Philipse, A. P. Direct Observation of Dipolar Chains in Iron Ferrofluids by Cryogenic Electron Microscopy. *Nat. Mater.* **2003**, *2*, 88–91.
8. Satoh, A.; Chantrell, R. W.; Coverdale, G. N.; Kamiyama, S. I. Stokesian Dynamics Simulations of Ferromagnetic Colloidal Dispersions in a Simple Shear Flow. *J. Colloid Interface Sci.* **1998**, *203*, 233–248.
9. Ilg, P.; Kröger, M.; Hess, S. Structure and Rheology of Model-Ferrofluids under Shear Flow. *J. Magn. Magn. Mater.* **2005**, *289*, 325–327.
10. Yamada, Y.; Enomoto, Y. A Microscopic Simulation for Structure Formation in Ferrofluid in Oscillatory Shear Flow. *AIP Conf. Proc.* **2006**, *832*, 337–340.
11. Wiedenmann, A.; Keiderling, U.; May, R. P.; Dewhurst, C. Dynamics of Field-Induced Ordering Processes in Ferrofluids Studied by Polarised Small-Angle Neutron Scattering. *Phys. B* **2006**, *385−386*, 453–456.
12. Pop, L. M.; Odenbach, S. Investigation of the Microscopic Reason for the Magnetoviscous Effect in Ferrofluids Studied by Small Angle Neutron Scattering. *J. Phys.: Condens. Matter* **2006**, *18*, S2785–S2802.
13. Promislow, J. H. E.; Gast, A. P.; Fermigier, M. Aggregation Kinetics of Paramagnetic Colloidal Particles. *J. Chem. Phys.* **1995**, *102*, 5492–5498.
14. Nguyen, Q. H.; Choi, S. B. Optimal Design of MR Shock Absorber and Application to Vehicle Suspension. *Smart Mater. Struct.* **2009**, *18*, No. 035012.
15. Chen, Z. Q.; Wang, X. Y.; Ko, J. M.; Ni, Y. Q.; Spencer, B. F.; Yang, G.; Hu, J. H. MR Damping System for Mitigating Wind−Rain Induced Vibration on Dongting Lake Cable-Stayed Bridge. *Wind Struct.* **2004**, *7*, 293–304.
16. Batterbee, D. C.; Sims, N. D.; Stanway, R.; Wolejsza, Z. Magnetorheological Landing Gear: 1. A Design Methodology. *Smart Mater. Struct.* **2007**, *16*, 2429–2440.
17. Birringer, R.; Wolf, H.; Lang, C.; Tschöpe, A.; Michels, A. Magnetic Nanorods: Genesis, Self-Organization and Applications. *Z. Phys. Chem.* **2008**, *222*, 229–255.
18. Larson, A. G. *The Structure and Rheology of Complex Fluids.*: Oxford University Press: New York, 1999.
19. O'Handley, R. C. *Modern Magnetic Materials: Principles and Applications;* John Wiley & Sons, Inc.: New York, 2000.
20. Wolf, H.; Sauer, H. M.; Birringer, R. Magnetic-Field-Induced Spontaneous Pattern Formation in Aerosol-Particle Deposits. *Europhys. Lett.* **2002**, *60*, 573–579.
21. Puntes, V. F.; Krishnan, K. M.; Alivisatos, A. P. Colloidal Nanocrystal Shape and Size Control: The Case of Cobalt. *Science* **2001**, *291*, 2115–2117.
22. Wang, C.; Hou, Y.; Kim, J.; Sun, S. A General Strategy for Synthesizing FePt Nanowires and Nanorods. *Angew. Chem., Int. Ed.* **2007**, *46*, 6333–6335.
23. Nielsch, K.; Castano, F. J.; Matthias, S.; Lee, W.; Ross, C. A. Synthesis of Cobalt/Polymer Multilayer Nanotubes. *Adv. Eng. Mater.* **2005**, *7*, 217–221.
24. Bachmann, J.; Jing, J.; Knez, M.; Barth, S.; Shen, H.; Mathur, S.; Gösele, U.; Nielsch, K. Ordered Iron Oxide Nanotube Arrays of Controlled Geometry and Tunable Magnetism by Atomic Layer Deposition. *J. Am. Chem. Soc.* **2007**, *129*, 9554–9555.
25. Samouhos, S.; McKinley, G. Carbon Nanotube−Magnetite Composites, with Applications to Developing Unique Magnetorheological Fluids. *J. Fluids Eng., Trans. ASME* **2007**, *129*, 429–437.
26. Butler, P. J. Self-Assembly of Tobacco Mosaic Virus: The Role of an Intermediate Aggregate in Generating Both Specificity and Speed. *Philos. Trans. R. Soc. London, B.* **1999**, *354*, 537–550.
27. Lewandowski, D. J. L. Genus Tobamovirus. In *Virus Taxonomy,* 8 ed.; Fauquet, C. M., Mayo, M. A., Maniloff, J., Desselberger, U., Ball, L. A., Eds.; Elsevier Academic Press: 2005; pp 1009−1014.
28. Namba, K.; Pattanayek, R.; Stubbs, G. Visualization of Protein-Nucleic Acid Interactions in a Virus. Refined Structure of Intact Tobacco Mosaic Virus at 2.9 Å Resolution by X-ray Fiber Diffraction. *J. Mol. Biol.* **1989**, *208*, 307–325.
29. Sachse, C.; Chen, J. Z.; Coureux, P. D.; Stroupe, M. E.; Fandrich, M.; Grigorieff, N. High-Resolution Electron Microscopy of Helical Specimens: A Fresh Look at Tobacco Mosaic Virus. *J. Mol. Biol.* **2007**, *371*, 812–835.
30. Mueller, A. Zielgerichtete Assemblierung Virusbasierter Biotemplate für die Nanotechnologie (Assembly of Virus-Derived Biotemplates Tailored to Nanotechnology Applications). Ph.D. Thesis, Universität Stuttgart, Stuttgart, 2009.
31. Demir, M.; Stowell, H. B. A Chemoselective Biomolecular Template for Assembling Diverse Nanotubular Materials. *Nanotechnology* **2002**, *13*, 541–544.
32. Royston, E.; Ghosh, A.; Kofinas, P.; Harris, M. T.; Culver, J. N. Self-Assembly of Virus-Structured High Surface Area Nanomaterials and Their Application as Battery Electrodes. *Langmuir* **2008**, *24*, 906–912.
33. Mueller, A.; Kadri, A.; Jeske, H.; Wege, C. *In Vitro* Assembly of Tobacco Mosaic Virus Coat Protein Variants Derived from Fission Yeast Expression Clones or Plants. *J. Virol. Methods* **2010**, *166*, 77–85.
34. Knez, M.; Sumser, M.; Bittner, A. M.; Wege, C.; Jeske, H.; Martin, T. P.; Kern, K. Spatially Selective Nucleation of Metal Clusters on the Tobacco Mosaic Virus. *Adv. Funct. Mater.* **2004**, *14*, 116–124.
35. Mutombo, K.; Michels, B.; Ott, H.; Cerf, R.; Witz, J. Scanning Calorimetric Studies of the Stability of Tobacco Mosaic Virus and Aggregates of its Coat Protein. *Eur. Biophys. J.* **1992**, *21*, 77–83.
36. Perham, R. N.; Wilson, T. M. A. The Characterization of Intermediates Formed During the Disassembly of Tobacco Mosaic Virus at Alkaline pH. *Virology* **1978**, *84*, 293–302.
37. Shenton, W.; Douglas, T.; Young, M.; Stubbs, G.; Mann, S. Inorganic−Organic Nanotube Composites from Template Mineralization of Tobacco Mosaic Virus. *Adv. Mater.* **1999**, *11*, 253–256.

38. Dujardin, E.; Peet, C.; Stubbs, G.; Culver, J. N.; Mann, S. Organization of Metallic Nanoparticles Using Tobacco Mosaic Virus Templates. *Nano Lett.* **2003**, *3*, 413–417.
39. Knez, M.; Kadri, A.; Wege, C.; Gösele, U.; Jeske, H.; Nielsch, K. Atomic Layer Deposition on Biological Macromolecules: Metal Oxide Coating of Tobacco Mosaic Virus and Ferritin. *Nano Lett.* **2006**, *6*, 1172–1177.
40. Knez, M.; Bittner, A. M.; Boes, F.; Wege, C.; Jeske, H.; Mai, E.; Kern, K. Biotemplate Synthesis of 3-nm Nickel and Cobalt Nanowires. *Nano Lett.* **2003**, *3*, 1079–1082.
41. Schlick, T. L.; Ding, Z.; Kovacs, E. W.; Francis, M. B. Dual-Surface Modification of the Tobacco Mosaic Virus. *J. Am. Chem. Soc.* **2005**, *127*, 3718–3723.
42. Yi, H.; Nisar, S.; Lee, S. Y.; Powers, M. A.; Bentley, W. E.; Payne, G. F.; Ghodssi, R.; Rubloff, G. W.; Harris, M. T.; Culver, J. N. Patterned Assembly of Genetically Modified Viral Nanotemplates *via* Nucleic Acid Hybridization. *Nano Lett.* **2005**, *5*, 1931–1936.
43. Tan, W. S.; Lewis, C. L.; Horelik, N. E.; Pregibon, D. C.; Doyle, P. S.; Yi, H. Hierarchical Assembly of Viral Nanotemplates with Encoded Microparticles *via* Nucleic Acid Hybridization. *Langmuir* **2008**, *24*, 12483–12488.
44. Sosnick, T.; Charles, S.; Stubbs, G.; Yau, P.; Bradbury, E. M.; Timmins, P.; Trewhella, J. Orienting Rigid and Flexible Biological Assemblies in Ferrofluids for Small-Angle Neutron Scattering Studies. *Biophys. J.* **1991**, *60*, 1178–1189.
45. SusTech GmbH. Vorrichtung zur Visualisierung von Magnetischen Feldern. (Developments for visualization of magnetic fields.) German Patent 203 12 398, 2003.
46. Zubarev, A. Y.; Fleischer, J.; Odenbach, S. Towards a Theory of Dynamical Properties of Polydisperse Magnetic Fluids: Effect of Chain-like Aggregates. *Phys. A* **2005**, *358*, 475–491.
47. Phule, P. P.; Ginder, J. M. Synthesis and Properties of Novel Magnetorheological Fluids Having Improved Stability and Redispersibility. *Int. J. Mod. Phys. B* **1999**, *13*, 2019–2027.
48. Odenbach, S. *Magnetoviscous Effects in Ferrofluids;* Springer: Berlin, 2002.
49. Devash, Y.; Hauschner, A.; Sela, I.; Chakraburtty, K. The Antiviral Factor (AVF) from Virus-Infected Plants Induces Discharge of Histidinyl-TMV-RNA. *Virology* **1981**, *111*, 103–112.
50. Fraenkel-Conrat, H.; Williams, R. C. Reconstitution of Active Tobacco Mosaic Virus from its Inactive Protein and Nucleic Acid Components. *Proc. Nat. Acad. Sci. U.S.A.* **1955**, *41*, 690–698.
51. Sambrook, R.; Russell, D. W. *Molecular Cloning: A Laboratory Manual,* 3rd ed.; Cold Spring Harbor Laboratory Press: Cold Spring Harbor, New York, 2001.
52. Crassous, J. J.; Regisser, R.; Ballauff, M.; Willenbacher, N. Characterization of the Viscoelastic Behavior of Complex Fluids Using the Piezoelastic Axial Vibrator. *J. Rheol.* **2005**, *49*, 851–863.
53. Kirschenmann, L. Aufbau Zweier Piezoelektrischer Sonden (PRV/ PAV) zur Messung der Viskoelastischen Eigenschaften Weicher Substanzen im Frequenzbereich 0.5 Hz−2 kHz bzw. 0.5 Hz−7 kHz. (Construction of Two Piezoelectric Probes (PRV/PAV) for the Measurement of Viscoelastic Properties of Soft Matter in the Frequency Ranges 0.5 Hz−2 kHz and 0.5 Hz−7 kHz, Respectively.) Ph.D. Thesis, Universität Ulm, Ulm, 2003.